J. theor. Biol. (1986) **118**, 101–113

A New Model for Biological Pattern Formation

PAUL MEAKIN

Central Research and Development Department, E. I. du Pont de Nemours and Company, Wilmington, DE 19898, *U.S.A.*

(*Received* 15 *April* 1985, *and in revised form* 19 *August* 1985)

Various non-equilibrium growth models have been used to explore the development of morphology in biological systems. Here we review a class of biological growth models which exhibit fractal structures and discuss the relationship of these models to a variety of other phenomena.

1. Introduction

A desire to obtain a better understanding of the development of morphology in biological systems has provided one of the main motivations for the study of non-equilibrium growth models. Much of our present understanding of non-equilibrium processes is a result of computer simulations carried out using simple models during the past two or three decades. This work has been encouraged by the observation that simple growth models can lead to complex behavior having some of the features characteristic of real systems. This is particularly true in the case of deterministic growth models (cellular automata) (Wolfram, 1983, 1984) which exhibit behavior paralleling that found in dissipative, nonlinear dynamic systems (Ott, 1981).

In this paper we are concerned with probabilistic growth models which can also lead to complex structures which mimic certain types of biological morphologies. These models lead to structures in which the fractal dimensionality, D (Mandelbrot, 1982), is distinctly smaller than the Euclidean dimensionality, d, of the space or lattice in which the growth process is occurring. For ordinary Euclidean objects, the dimensionality, d, is the exponent which describes how the mass of the object, M, scales with some characteristic length l which describes the overall size

$$M \sim l^d. \tag{1}$$

In this case d is an integer (3 for a sphere, 2 for a plane and 1 for a line). Many objects are found in nature (Mandelbrot, 1982) for which the form of the mass–length scaling relationship given in equation (1) is preserved but the exponent is no longer equal to the Euclidean dimensionality of the embedding space in which the object exists

$$M \sim l^D. \tag{2}$$

In this case the exponent D is called the fractal dimensionality (Mandelbrot, 1982). In general D is not an integer and satisfies the condition $D < d$. However, in some

0022-5193/86/010101+13 $03.00/0

cases (such as a random walk) D may have an integer value (D has a value of 2·0 for random walks in a space of any Euclidean dimensionality).

The mass-length scaling relationship given in equation (2) is the basis for all methods to measure the fractal dimensionality of real objects or objects generated in computer simulations. For computer simulations of nonequilibrium growth and aggregation processes three mass-length scaling relationships are commonly used to measure the fractal dimensionality. These are

$$R_g \sim N^{(1/D_\beta)} \tag{3a}$$

$$M(l) \sim l^{D_\gamma} \tag{3b}$$

and

$$C(r) \sim r^{(D_\alpha - d)}. \tag{3c}$$

In equation (3a) R_g is the radius of gyration and N is the mass (number of particles or occupied lattice sites) of the growing object. In equation (3b) $M(l)$ is the mass contained within the distance l measured from some occupied site (generally l is measured from the initial growth site or "seed"). In equation (3c) $C(r)$ is the two point density-density correlation function at a distance r. For all real systems and systems generated by finite size simulations these mass-length scaling relationships are obeyed over only a finite range of length scales bounded by upper and lower cut offs. Consequently, the exponents D_α, D_β and D_γ are effective fractal dimensionalities. In the asymptotic limit (where the range of length scales becomes infinite) D_α, D_β and D_γ converge on a common value D which is the fractal dimensionality. Besides obeying equation (2) fractals also display the property of self-similarity (or statistical self-similarity in the case of random fractals). In other words they are scale invariant and look the same under different magnifications. As in the case of the mass-length scaling relationships, this property of self-similarity does not extend over an infinite range of length scales for real systems.

Since, in general, $D < d$ for real fractal objects, the mean density of fractal objects becomes smaller and smaller as they grow larger and larger. Fractals contain holes or gaps covering a wide range of length scales up to the overall size of the fractal. These characteristics can be seen in the results of most of our simulations.

One of the earliest examples of probabilistic growth models is the "Eden" (Eden, 1961) model (Fig. 1) in which each vacant surface site has the same probability of becoming occupied at all stages of growth. This model generates compact structures in which the fractal dimensionality (Mandelbrot, 1982) D is equal to the Euclidean dimensionality d. A closely related model which includes competing growth and decay process was developed by Williams & Bjerknes (1972) as a model for the growth of skin cancer. They found that for their model the "surface" perimeter size S depended on the total mass or number of occupied sites in the cluster N according to the power law relationship

$$S = N^{0.55}. \tag{4}$$

This result suggested that the surface of Williams-Bjerknes (1972) clusters may have a fractal geometry. However, more recent work with this model (Peters *et al.*, 1979;

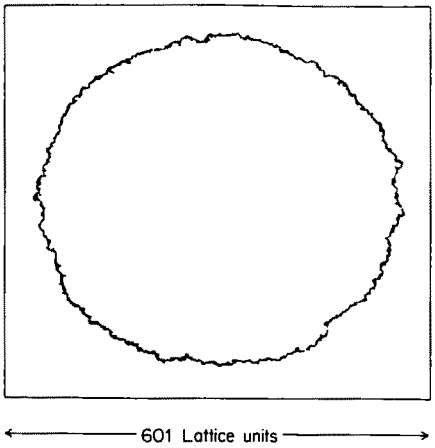

FIG. 1. The 2372 unoccupied interface sites associated with a 200000 site cluster grown using the Eden model.

Meakin, unpublished) suggests that the surface is rough but not fractal-like. This conclusion is supported by the theoretical work of Richardson (1973). Figure 2 shows a 100 000 site Williams-Bjerknes (1972) cluster grown with a "carcinogenic advantage" of 1·1. The carcinogenic advantage is equal to the growth probability divided by the decay probability.

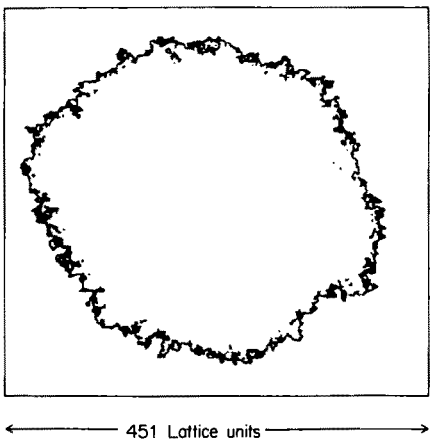

FIG. 2. The 4135 unoccupied interface sites associated with a 100000 site cluster grown using the Williams-Bjerknes model with a carcinogenic advantage of 1·1. The advantage is equal to (growth probability)/(decay probability). The surface of this cluster appears to be rough but not fractal.

In recent years a variety of biological growth models have been studied (Tautu, 1978; MacDonald, 1983; Gierer & Meinhardt, 1972; Gierer, 1980; Meinhardt, 1982), but, to our knowledge, none of these leads to structures with well-defined fractal dimensionality. For example, the network formation model of Meinhardt (1982)

generates a uniform (non-fractal) network of occupied lattice sites leading to the type of structure shown in Fig. 3. The morphology shown in this figure results from a combination of non-linear chemical reaction processes and diffusion. Models of this type may lead to fractal structures under some conditions but so far these conditions have not been found.

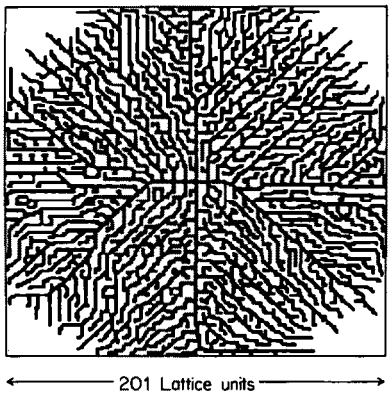

FIG. 3. A growth of 8909 occupied lattice sites generated using Meinhardt's "network" model. This model generates a network of occupied lattice sites which is uniform on all but short length scales. The structure is not a fractal. A detailed discussion of the model is given by Meinhardt (1982).

Recently interest in non-equilibrium growth processes has been stimulated by the demonstration by Witten & Sander (1981) that structures with a well-defined fractal geometry are generated by a simple diffusion limited aggregation process in which particles are added one at a time to a growing cluster or aggregate via random walk trajectories. This model has generated considerable theoretical interest (Gould *et al.*, 1983; Muthukumar, 1983; Nauenberg, 1983; Nauenberg *et al.*, 1983; Deutch & Meakin, 1983; Hentschel, 1984) and has led to the development of a number of more or less closely related models (Rikvold, 1982; Meakin, 1983*a*, *b*; Kolb *et al.*, 1983; Niemeyer *et al.*, 1984) which also generate fractal structures. It has also stimulated experimental investigations (Brady & Ball, 1984; Matsushita *et al.*, 1984). A typical two-dimensional Witten-Sander cluster is shown in Fig. 4.

Since the growth of many biological systems may be limited by the diffusion of nutrients to the system or the diffusion of toxic metabolites away from the system, the diffusion limited aggregation model of Witten & Sander (1982) may provide new insight into the morphology of certain biological systems.

The model which we discuss below is similar to the Eden model in that growth occurs by the random occupation of vacant surface sites. However, we assume that the rate of growth (growth probability) depends on the local concentration of some substance which diffuses from a surrounding exterior source and is consumed by the growing system. If the process is diffusion limited, and if the rate of growth is directly proportional to the local nutrient concentration, our model becomes very similar to the Witten-Sander (1982) model. In this case a structure with a fractal dimensionality of about 1·7 is formed in $2d$ simulations (Witten & Sander, 1982,

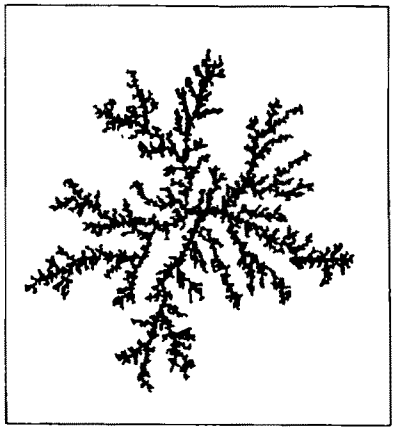

FIG. 4. An aggregate of 10 000 particles obtained from an off lattice version of the Witten-Sander model for diffusion limited aggregation. This structure, which is in a two-dimensional space, is a random fractal with a fractal dimensionality of about 5/3.

1983), and in three dimensions a structure with a fractal dimensionality of about 2·5 is obtained (Meakin, 1983*c*,*d*).

If the growth probability (p) is proportional to some power (ε) of the local concentration (c)

$$P \sim c^{\varepsilon} \tag{5}$$

then our model becomes equivalent to the dielectric breakdown model which was developed by Niemeyer *et al.* (1984). In this case the fractal dimensionality generated by the model depends on the exponent ε and may vary from 1·0 to d, the Euclidean dimensionality of the space in which the growth process is embedded.

2. The Model

Our simulations are carried out on a two-dimensional square lattice. We start with a single occupied lattice site surrounded by a low concentration of nutrient and an exterior source of nutrient. The nutrient is supplied by the boundary conditions which maintain a fixed concentration ($c = 1{\cdot}0$) of nutrient on a circle of lattice sites surrounding the growing cluster. Initially this circle has a radius of 15 lattice units, but it grows with the cluster such that its radius is always significantly larger than the maximum radius of the cluster R_{max}. In most of our simulations the nutrient is supplied at a distance of $2{\cdot}0R_{max}$ or $2{\cdot}5R_{max}$ from the origin of the growth. Figure 5 gives a schematic representation of the early stages of one of the simulations.

In the most simple version of the model we assume that a nutrient concentration of zero is maintained on the lattice sites occupied by the cluster at all times and that the diffusion process is fast compared to the growth process. Under these conditions, the concentration field will reach a steady state determined by the

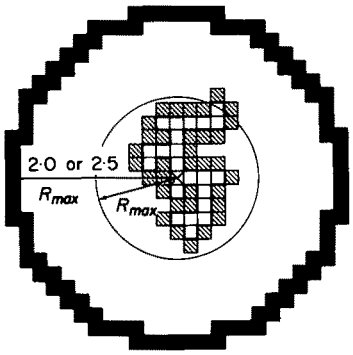

FIG. 5. A schematic representation of a simulation of diffusion limited growth at an early stage in the simulation. The concentration inside the filled lattice sites is 1·0, and the concentration inside the open lattice sites, which constitute the cluster, is 0. □ occupied site, $c = 0{\cdot}0$; ▨ boundary, $c = 1{\cdot}0$; ▧ potential growth site.

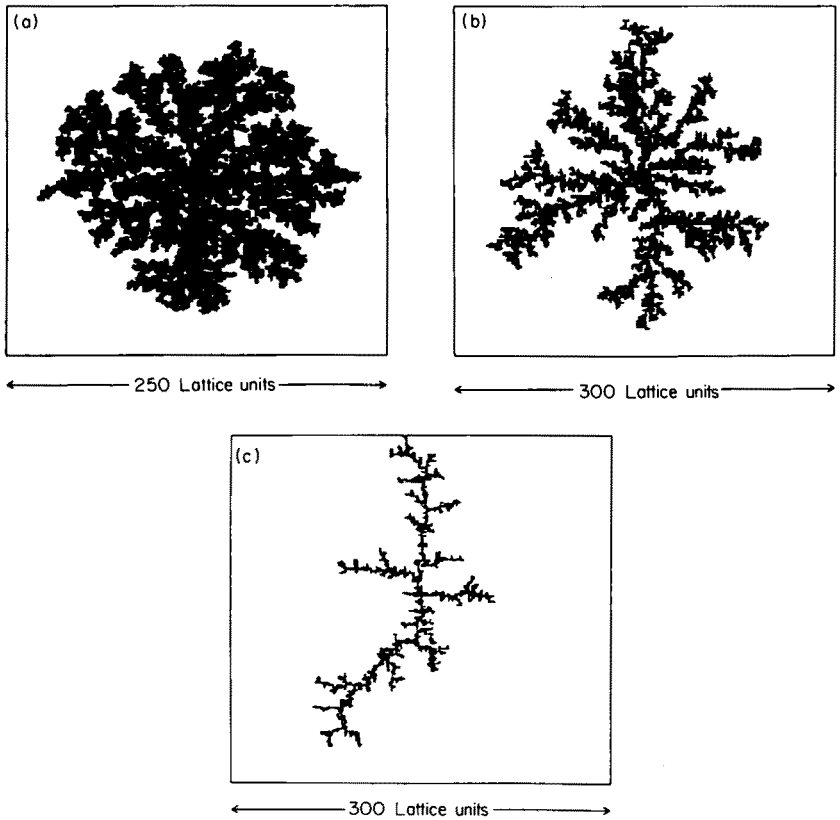

FIG. 6. Typical clusters generated with growth exponents ε of 0·5, 1·0 and 2·0. (a) Shows a cluster of 12 000 sites generated with a value of 0·5 for ε. (b) Shows a cluster of 8000 sites generated with ε set to a value of 1·0. (c) Shows a cluster of 2126 sites obtained using a value of 2·0 for the growth exponent.

boundary conditions before each growth event, i.e.

$$\frac{dc}{dt} = \mathscr{D}\nabla^2 c = 0 \tag{6}$$

where $\mathscr{D}$ is the diffusion coefficient.

In order to approximate the conditions $\nabla^2 c = 0$ before each growth step, the concentration field is "relaxed" by replacing the concentration on each lattice site by the average of the concentrations on the four nearest neighbor lattice sites. In most of our simulations this process is repeated 10 or 20 times before each growth step. Within the statistical uncertainties of our simulations our results do not seem to depend on whether 10 or 20 relaxation stages are used or whether the source of nutrient is placed at a distance of 2·0 or $2{\cdot}5R_{max}$.

At each growth step unoccupied surface sites are picked at random and a random number in the range $0 < x < 1$ is generated. If $x < c^{\varepsilon}$ (where c is the nutrient concentration at that site), then the site is occupied and growth has occurred. If $x > c^{\varepsilon}$, another site is picked at random and tested. The procedure is repeated until a growth event occurs. The sequence of relaxation and growth processes is repeated until a large cluster has grown. In typical simulations, clusters were grown to a size of about 12 000 occupied lattice sites for $\varepsilon = 1{\cdot}0$ and about 2000–2500 for $\varepsilon = 2{\cdot}0$. Typical clusters generated in this manner are shown in Fig. 6.

3. Results

The fractal dimensionalities of the clusters generated using growth exponents ε of 0·5, 1·0 and 2·0 were estimated from both the dependence of the radius of gyration on cluster size (effective dimensionality D_{β}, equation (3a)) (Stanley, 1977) and from the density-density correlation function (effective dimensionality D_{α}, equation (3c)) (Witten & Sander, 1982). Figure 7 shows the density-density correlation functions averaged for five clusters generated using a growth exponent ε of 2·0. An effective fractal dimensionality D_{α} can be obtained using the expression

$$D_{\alpha} = d + d \ln (C(r))/d \ln (r) \tag{7}$$

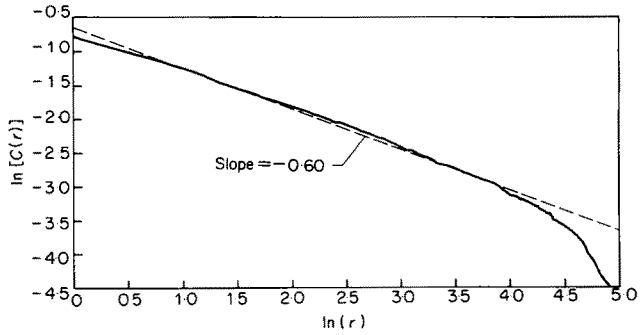

FIG. 7. The average density-density correlation function $C(r)$ obtained from five simulations of diffusion limited growth with a growth probability exponent ε of 2·0. The slopes of −0·6 associated with the linear region in this log-log plot gives a fractal dimensionality of $d - 0{\cdot}6$ or $\simeq 1{\cdot}4$.

where $C(r)$ is the density-density correlation function at a distance r. Equation (7) is applicable at intermediate length scales where $\ln(C(r))$ depends linearly on r. The results shown in Fig. 7 indicate that D_α has a value of about 1·4. Our results for both D_α and D_β are summarized in Table 1.

TABLE 1

Fractal dimensionalities obtained using the diffusion limited growth model. The effective dimensionality D_α was obtained from the density-density correlation function, and D_β was obtained from the dependence of the radius of gyration on the mass of the growth. To obtain estimates for D_α straight lines were least squares fitted to the co-ordinates $(ln(C(r)), (ln(r))$ over the range $2 \leq r \leq 20$ lattice units. A similar procedure was used to obtain the effective dimensionality D_β using the co-ordinates $(ln(R_g)), (ln(N))$ over the ranges of cluster sizes shown. N_{max} is the total number of occupied sites at the end of the simulation

Growth exponent ε	D_α $2 \leq r \leq 20$	D_β $0{\cdot}1N_{max} \leq N \leq N_{max}$	D_β $0{\cdot}5N_{max} \leq N \leq N_{max}$
0·5	1·86 ± 0·02	1·92 ± 0·05	1·94 ± 0·04
1·0	1·71 ± 0·02	1·72 ± 0·06	1·70 ± 0·08
2·0	1·44 ± 0·02	1·39 ± 0·10	1·36 ± 0·05
1·0 (method 2)	1·69 ± 0·02	1·78 ± 0·06	1·69 ± 0·07

As a check on the numerical average of our simulations they were repeated for the case $\varepsilon = 1{\cdot}0$ using a procedure in which the concentration field was updated until the concentration in each unoccupied site next to an occupied site (i.e. each potential growth site) changed by less than 0·1% per iteration. The results of these simulations, identified as method 2, are also shown in Table 1.

For the case $\varepsilon = 1{\cdot}0$ our results are in good agreement with those obtained by Niemeyer *et al.* (1984) for the equivalent dielectric breakdown model and with results obtained earlier using the Witten-Sandar model for diffusion limited aggregation (Witten & Sander, 1982; Meakin, 1983*c*,*d*). However, a comparison of Fig. 6(b) with simulations carried out on a $2d$ square lattice using the Witten-Sander model for diffusion limited aggregation with a sticking probability of 1·0 indicated that the short length scale structure is not the same in these two models. For $\varepsilon = 0{\cdot}5$ our results are in good agreement with those of Niemeyer *et al.*, but for $\varepsilon = 2{\cdot}0$ we estimate a fractal dimensionality of about 1·4 which is somewhat smaller than the estimate of about 1·6 obtained by Niemeyer *et al.*

4. Boundary Conditions

We do not expect that a change in boundary conditions will be sufficient to change the fractal dimensionality of structures generated by the diffusion limited growth model discussed above. However, a change in the boundary conditions from those associated with the model used to generate the results shown in Fig. 6 and Table 1

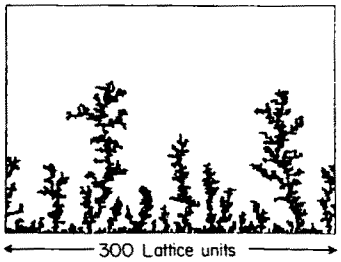

FIG. 8. The results of a small scale simulation of diffusion limited deposition. In this $2-d$ simulation, particles were deposited onto the lower "surface" with a sticking probability of 1·0.

may lead to interesting and potentially important new effects in the same way that diffusion limited deposition on fibers and surfaces (Meakin, 1983*e*) leads to new quantities (cluster size distributions for example) (Racz & Vicsek, 1983) which are not found in diffusion limited aggregation on single growth sites. Figure 8 shows the results of two-dimensional simulations of diffusion limited deposition taken from Meakin (1983*e*).

Similar simulations can be carried out with the diffusion limited growth model with the added flexibility that the growth probability exponent (ε) can be varied, and deposits with any fractal dimensionality in the range $1{\cdot}0 \leq D \leq d$ can be

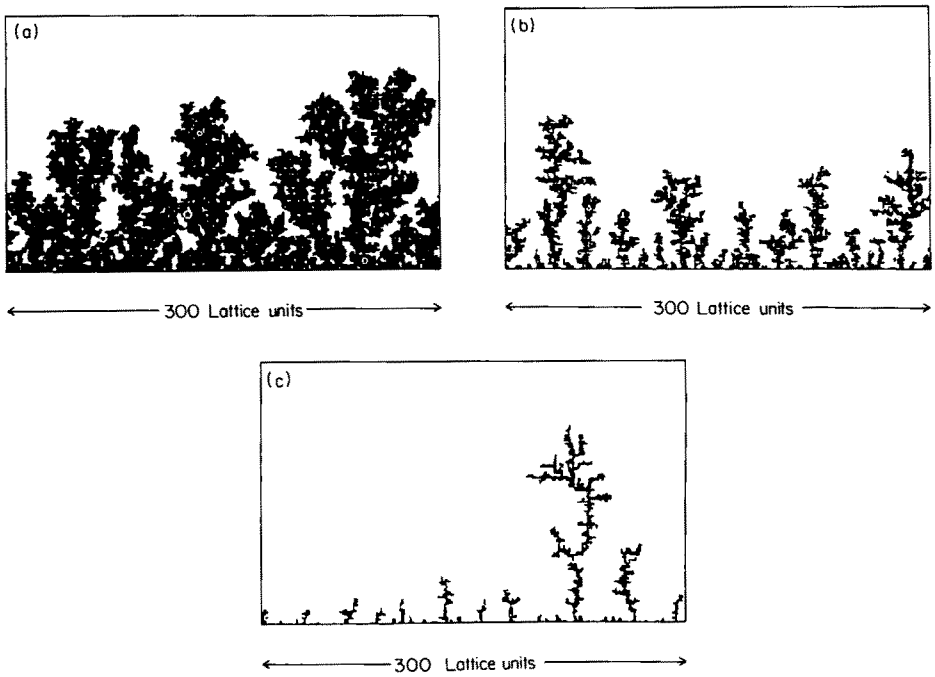

FIG. 9. Diffusion limited growth from a "surface." In these simulations any site adjacent to the "surface" on some part of the "growth" was considered to be a potential growth site. (a), (b) and (c) Show the results obtained with growth probability exponents (ε) of 0·5, 1·0 and 2·0, respectively.

generated. The simulations were carried out on 300×300 square lattices. The concentration in the "top" row of lattice sites was fixed at a value of 1·0, and the concentration in the bottom row was fixed at a value of 0·0. Any unoccupied site adjacent to a site in the lower boundary or in the growing "deposit" was considered to be a potential growth site. Periodic boundary conditions were used at the sides of the two-dimensional lattice. Results obtained using this model are shown in Fig. 9. To obtain the results shown in Fig. 9, the growth process was stopped when the deposit had grown to maximum height of 150 lattice units.

Figure 10 shows the results obtained from a similar model in which only one of the sites in the lower row is initially able to grow. Sites adjacent to this "seed" site or adjacent to a site on the growing "tree" are considered to be potential growth sites.

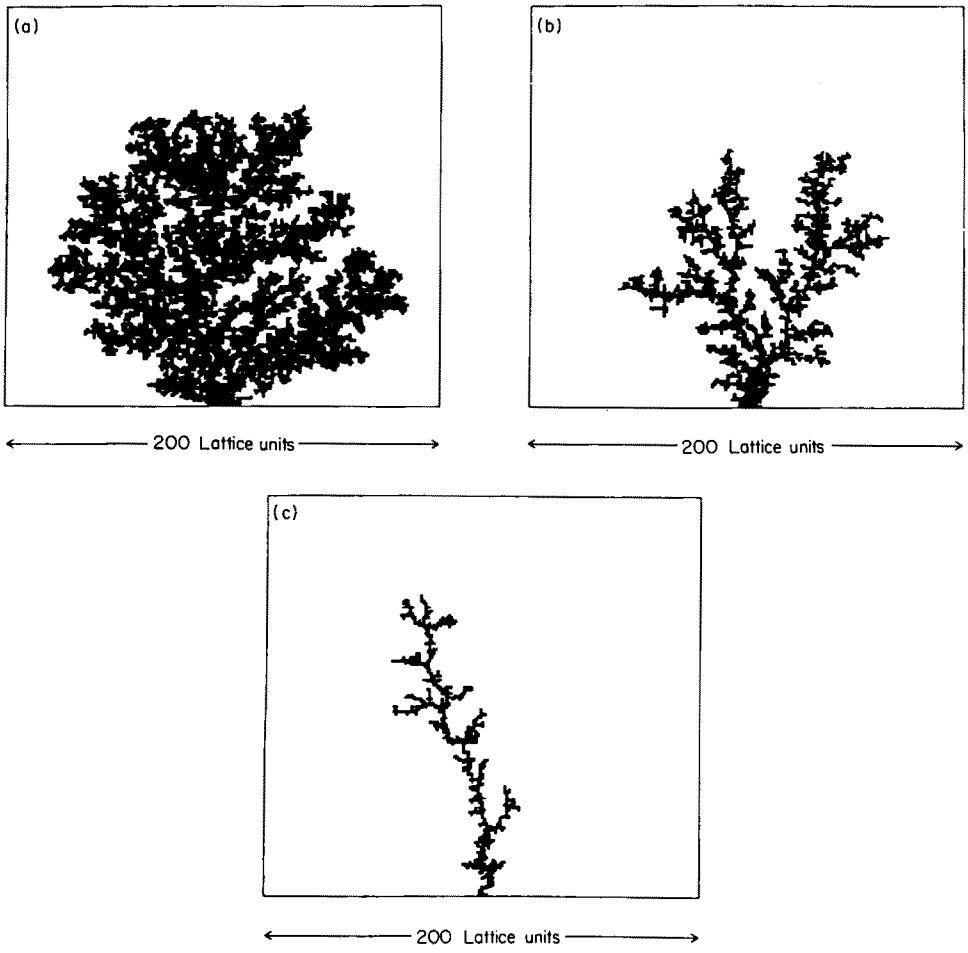

FIG. 10. The model used to obtain these figures is similar to that used to generate Fig. 9. However, in this case only one site in the bottom row is capable of growth (the middle site). (a), (b) and (c) Show the results obtained with growth probability exponents of 0·5, 1·0 and 2·0, respectively.

For those cases where the growth probability exponent is sufficiently large, the "surface growths" shown in Fig. 9 consist of a number of independent trees. A similar characteristic can be seen in simulations of diffusion limited aggregation with multiple growth sites (Witten & Meakin, 1983). In this case aggregates growing from nearby growth sites or seeds do not join because the region between two clusters is screened from particle penetration. Similarly, the region between two nearby growths generated by the diffusion limited growth model will also be screened from the concentration field, and growth will not occur in this region. To demonstrate this effect, simulations have been carried out with two growth sites separated by 10 lattice units (Fig. 11). In these simulations the source of nutrient material was represented by a fixed concentration of 1·0 at a distance of 3 R_{max} from the origin

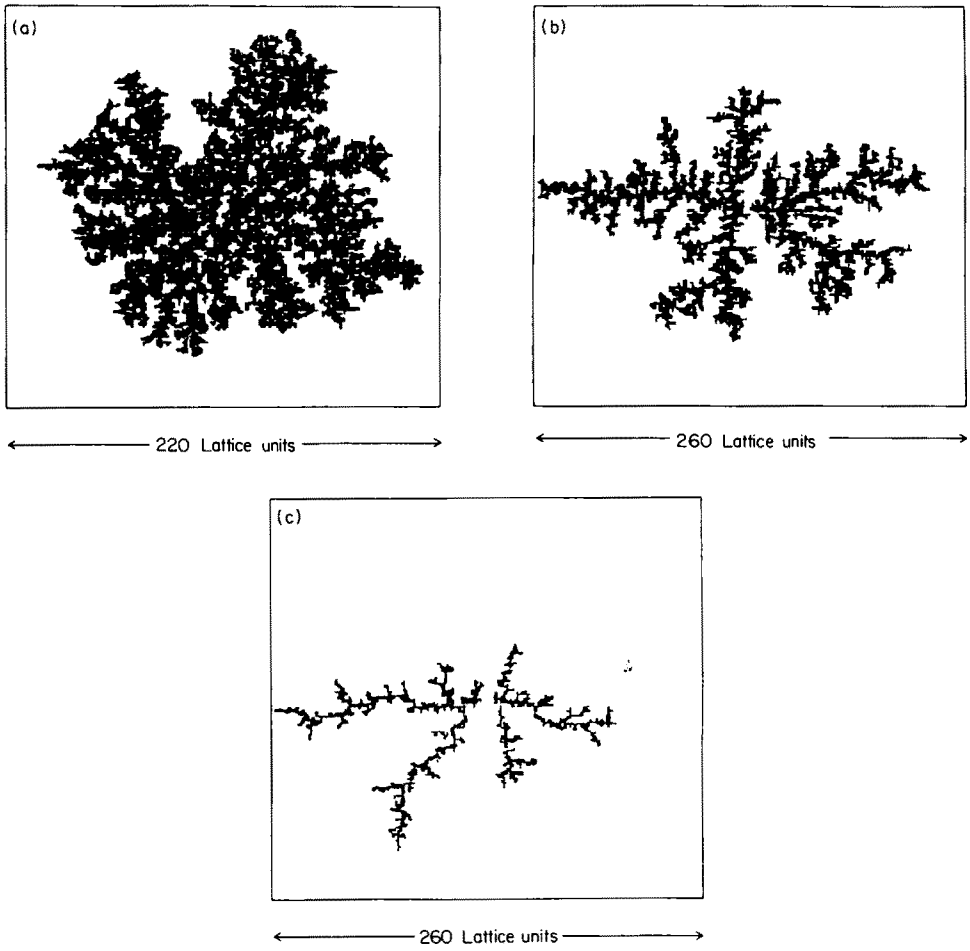

FIG. 11. Diffusion limited growth from two growth sites or seeds separated by 10 lattice units. The results shown in (a), (b) and (c) were obtained with growth probability exponents ε of 0·5, 1·0 and 2·0, respectively.

of the lattice. Here R_{max} is the distance from the origin (between the two growth sites) to the most distant occupied lattice site in either cluster. For the cases $\varepsilon = 1{\cdot}0$ and $\varepsilon = 2{\cdot}0$ the growths from the two nearby growth sites do not join. For the case $\varepsilon = 0{\cdot}5$ the screening effects are too weak to prevent the two growths from joining.

We have also carried out simulations of diffusion controlled growth with a point source of nutrient. In these simulations the boundary conditions are specified by maintaining a concentration of 1·0 on the source site and a concentration of 0·0 on the sites occupied by the growth. Absorbing boundary conditions $\varepsilon = 0{\cdot}0$ are also maintained at a distance of 3 R_{max} from the center of the lattice (located at the end point between the nutrient source and the growth site). Figure 12 shows some results obtained from this model.

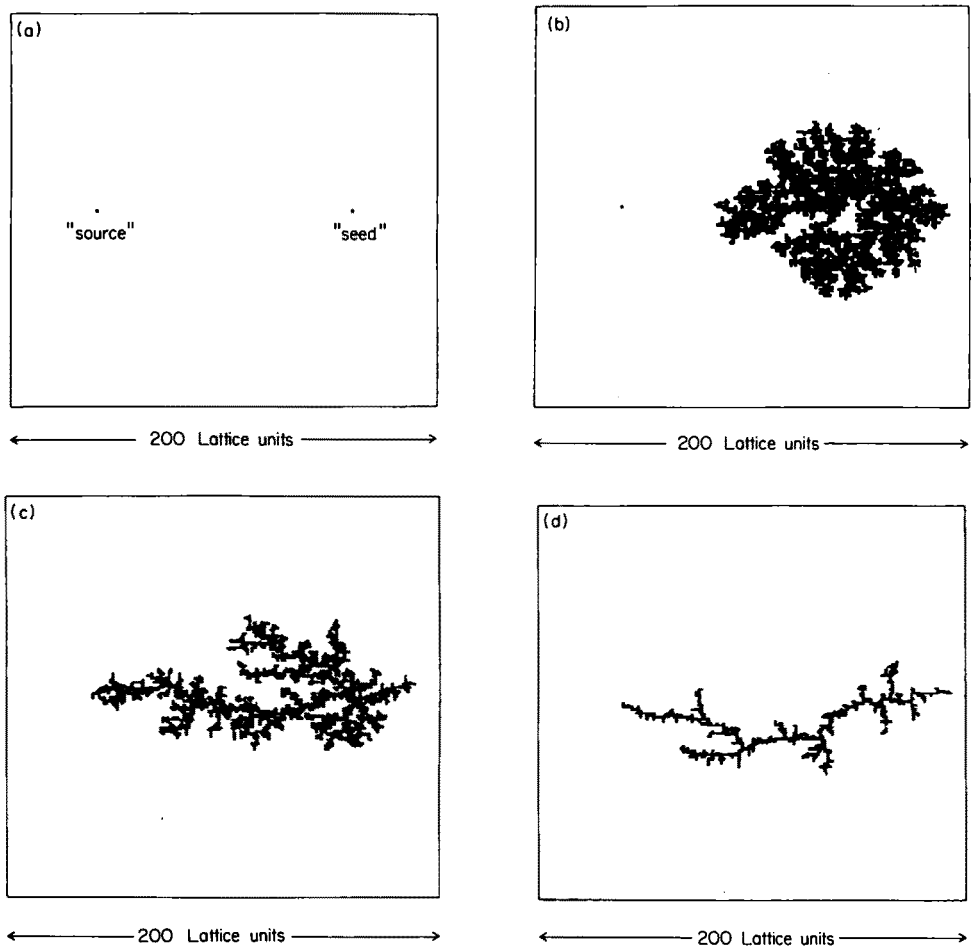

FIG. 12. Diffusion limited growth with a point source of nutrient. (a) Shows the locations of the source and the seed. (b), (c) and (d) Show results obtained with growth probability exponents of 0·5, 1·0 and 2·0, respectively. The source and seed sites are separated by 120 lattice units.

Patterson (1984) has pointed out that the diffusion limited aggregation model of Witten & Sander (1982) can be used to model two fluid displacement in porous media. Our simulations with a point source of nutrient are similar to his simulations. The additional parameter in our model ε may allow some of the specific properties of the two fluids to be taken into account such as the rheology of the two fluids.

The author wishes to acknowledge useful discussions with D. J. Scalapino.

REFERENCES

BRADY, R. & BALL, R. C. (1984). *Nature* **309**, 225.
DEUTCH, J. M. & MEAKIN, P. (1983). *J. chem. Phys.* **78**, 2093.
EDEN, M. (1961). In: *Proc. Fourth Berkeley Symposium on Mathematics, Statistics and Probability* (Neeyman, J. ed.). Vol. IV, p. 223. Berkeley: University of California Press.
GIERER, A. & MEINHARDT, H. (1972). *Kybernetik* **12**, 30.
GIERER, A. (1980). *Prog. Biophys. Molec. Biol.* **37**, 1.
GOULD, H., STANLEY, H. E. & FAMILY, F. (1983). *Phys. Rev. Lett.* **50**, 686.
HENTSCHEL, H. G. E. (1984). *Phys. Rev. Lett.* **52**, 212.
KOLB, M., BOTET, R. & JULLIEN, R. (1983). *Phys. Rev. Lett.* **51**, 1123.
MACDONALD, N. (1983). *Trees and Networks in Biological Models.* New York: Wiley & Sons.
MATSUSHITA, M., SANO, M., HAYAKAWA, Y., HONJO, H. & SAWADA, Y. (1984). *Phys. Rev. Lett.* **53**, 286.
MEAKIN, P. (1983*a*). *Phys. Rev. B* **28**, 6718.
MEAKIN, P. (1983*b*). *Phys. Rev. Lett.* **51**, 1119.
MEAKIN, P. (1983*c*). *Phys. Rev. A* **27**, 604.
MEAKIN, P. (1983*d*). *Phys. Rev. A* **27**, 1495.
MEAKIN, P. (1983*e*). *Phys. Rev. A* **27**, 2616.
MEINHARDT, H. (1982). *Models of Biological Pattern Formation.* New York: Academic Press.
MANDELBROT, B. B. (1982). *The Fractal Geometry of Nature* (1982). San Francisco: Freeman & Co.
MUTHUKUMAR, M. (1983). *Phys. Rev. Lett.* **50**, 839.
NAUENBERG, M. (1983). *Phys. Rev. B* **28**, 449.
NAUENBERG, M., RICHTER, R. & SANDER, L. M. (1983). *Phys. Rev. B* **28**, 1649.
NIEMEYER, L., PIETRONERO, L. & WIESMANN, H. J. (1984). *Phys. Rev. Lett.* **52**, 1033.
OTT, E. (1981). *Rev. Mod. Phys.* **53**, 655.
PATTERSON, L. (1984). *Phys. Rev. Lett.* **52**, 1621.
PETERS, H. P., STAUFFER, D., HÖLTERS, H. P. & LOEWENICH, K. (1979). *A. Physik B* **34**, 399.
RACZ, Z. & VICSEK, T. (1983). *Phys. Rev. Lett.* **51**, 2382.
RICHARDSON, D. (1973). *Proc. Comb. Philos. Soc.* **74**, 515.
RIKVOLD, P. A. (1982). *Phys. Rev. A* **26**, 647.
STANLEY, H. E. (1977). *J. Phys. A* **10**, L211.
TAUTU, P. (1978). *Z. Kresbforsch* **91**, 223.
WILLIAMS, T. & BJERKNES, R. (1972). *Nature* **236**, 19.
WITTEN, T. A. & SANDER, L. M. (1981). *Phys. Rev. Lett.* **47**, 1400.
WITTEN, T. A. & SANDER, L. M. (1983). *Phys. Rev. B* **27**, 5686.
WITTEN, T. A. & MEAKIN, P. (1983). *Phys. Rev. B* **28**, 5632.
WOLFRAM, S. (1983). *Rev. Mod. Phys.* **55**, 601.
WOLFRAM, S. (1984). *Nature* **311**, 419.